Paper submitted to the ASME/AIChE/ANS National Heat Transfer Conference, Session on Fundamentals of Severe Accident Analysis, Philadelphia, PA, August 6-10, 1989.

CONF-890819--21

DE89 017687

IMPINGEMENT HEAT FLUX BY DISPERSED MOLTEN METAL FUEL ON A HORIZONTAL STAINLESS STEEL STRUCTURE*

by

J. D. Gabor, R. T. Purviance, R. W. Aeschlimann, and B. W. Spencer

Reactor Analysis and Safety Division
Argonne National Laboratory
9700 S. Cass Ave.
Argonne, IL 60439

*Work sponsored by U. S. Department of Energy, Technology Support Programs.

IMPINGEMENT HEAT FLUX BY DISPERSED MOLTEN METAL FUEL ON A HORIZONTAL STAINLESS STEEL STRUCTURE

by

J. D. Gabor, R. T. Purviance, R. W. Aeschlimann, and B. W. Spencer

ABSTRACT

Although the Integral Fast Reactor (IFR) possesses inherent safety features, an assessment of the consequences of melting of the metal fuel is necessary for risk analysis. As part of this effort an experimental study was conducted to determine the depths of sodium at 600 C required for pour streams of various molten uranium alloys (U, U-5 wt% Zr, U-10 wt% Zr, and U-10 wt% Fe) to break up and solidify. The quenched particulate material, which was in the shape of filaments and sheets, formed coolable beds because of the high voidage (~0.9) and large particle size (~10 mm). In a test with a 0.15-m sodium depth, the fragments from a pure uranium pour stream did not completely solidify but formed an agglomerated mass which did not fuse to the base plate. However, the agglomerated fragments of U-10 wt% Fe eutectic fused to the stainless steel base plate. An analysis of the temperature response of a 25-mm thick base plate was made by volume averaging the properties of the sodium and metal phases and assuming two semi-infinite solids coming into contact. Good agreement was obtained with the data during the initial 5 to 10 s of the contact period.

Introduction

Important design features of the Integral Fast Reactor (IFR) are (1) its pool configuration which facilitates passive decay heat removal and isolates the core from exterior components, (2) inherent shutdown capability, and (3) the use of a metallic fuel with superior heat transfer properties compared to oxide fuels. Although the IFR possesses these inherent safety features, an assessment of the consequences of melting of the metallic fuel is necessary for a comprehensive risk analysis.

The breakup of jets and drops of molten metals in various liquids other than uranium alloys in sodium have been studied by numerous investigators. These studies have generally been on a gram scale except for aluminum and mixed oxides produced by thermite reactions.[1-9] Jet-impingement surface

ablation and heat transfer is a subject of considerable interest in severe core-melt accidents.[10,11] However, the mechanism and extent of impingement attack by uranium alloy pour streams in sodium have been undetermined. Therefore a study has been undertaken to determine the depth of sodium required for a pour stream of molten metallic fuel to break up and solidify and the subsequent heat transfer and melt attack on a horizontal stainless steel surface by the pour stream material that has not frozen.[12,13]

Experimental

The tests consisted of inductively melting kilogram quantities of uranium alloys in a MgO crucible and removing a ZrO plug to initiate a downward pour of the melt into a pool of 600 C sodium. The tests were conducted with the apparatus shown on Fig. 1 which essentially consisted of a furnace/injector for melting the pour stream metals, an interaction vessel containing the sodium, and an overall containment vessel. Thermocouples spaced 152 mm apart indicated the temperature profile of the sodium pool. A 30-kW, 10,000 Hz TOCCO motor generator was used. The sodium was contained in heated 192-mm ID interaction vessels of variable length with argon cover gas. For tests with shallow sodium pools in which impingement heat transfer occurred, a thermocouple was located at the center on the top surface of a 25.4-mm thick base plate and three thermocouples were located at 6.4-mm intervals within the base plate.

Results

The parameters and resulting fragment beds of the tests are summarized in Table 1. The uranium pour streams broke up and the fragments were frozen when reaching the base plate for sodium depths as low as 0.3 m. In the tests with deeper sodium pools the pour streams under gravitational acceleration (2 m/s velocity) typically fragmented into particles of about 10 mm in mean size, which settled to form a bed having a voidage in the order of 0.9. A debris bed with these characteristics formed from a meltdown of a metal-fuel pool reactor would be largely coolable by conduction. Extraordinarily high bed depths could be accommodated before bed dryout even if boiling occurred because the high voidage of the bed offers little resistance to convective flow.[12]

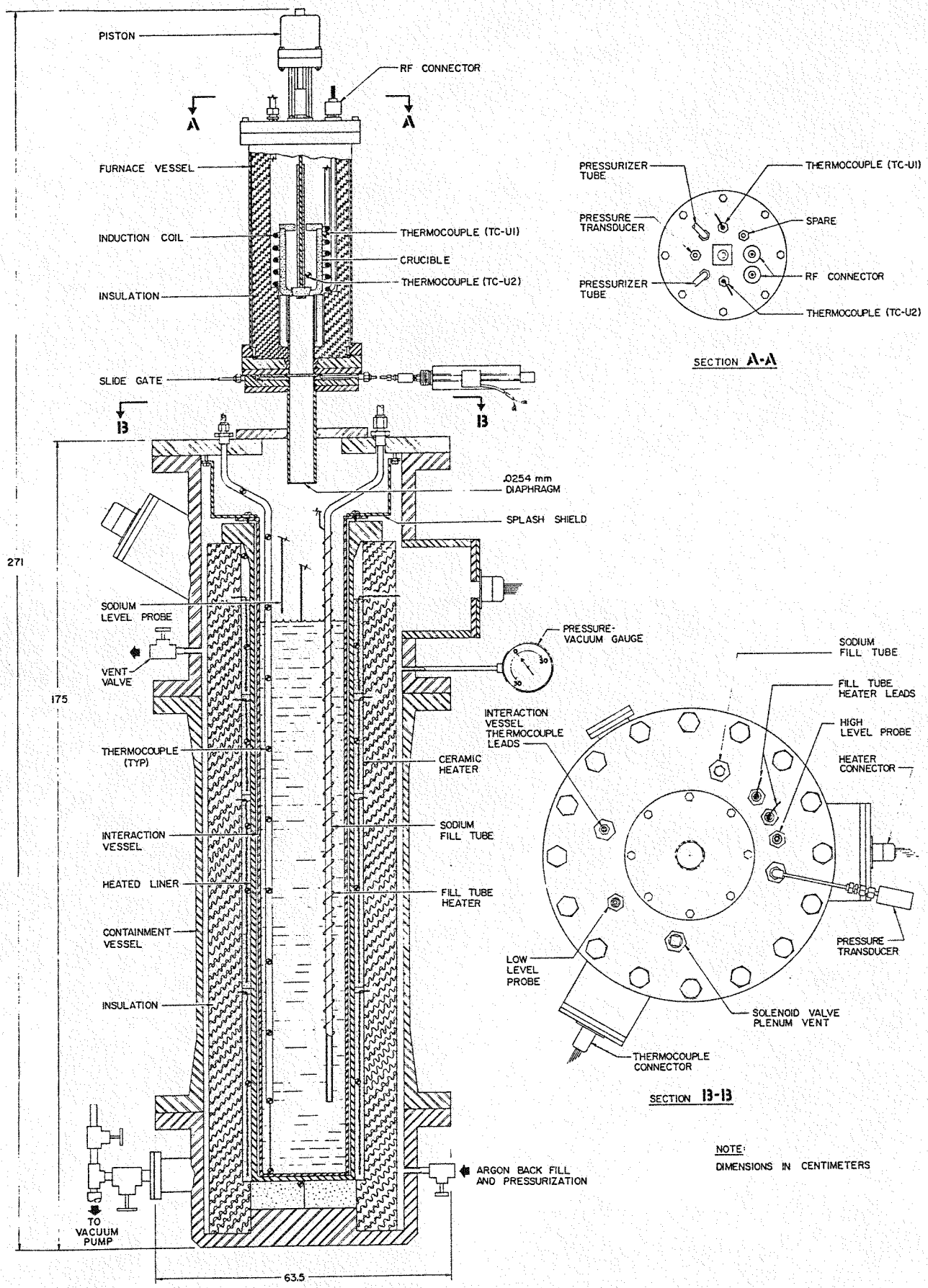

Fig. 1. Apparatus for Pour Stream Breakup Experiments.

TABLE 1. Pour Stream Breakup Experiments Sodium Temperature at 600 C

Test	Melt Material	Melt[a] Superheat, °C	Injection Velocity, m/s	Injection Diameter, mm	Melt wt, kg	Sodium Depth, m	Bed Void Fraction	Particle Size, mm[c]
2	U	100	2	25	2.98	1.2	0.95	16.13
3	U-10Zr	100	2	25	2.99	1.2	0.95	9.68
4	U-5Zr	100	2	25	3.01	1.2	0.95	10.54
5	U-5Zr	10	2	25	3.00	1.2	0.97[b]	13.71
6	U-5Zr	300	2	25	3.01	1.2	0.94	8.16
7	U-5Zr	100	2	12.5	3.00	1.2	0.96	7.60
8	U-5Zr	100	10	25	3.00	1.2	0.84	0.59
9	U	400	2	25	3.01	0.9	0.90	8.59
10	U	400	2	25	3.01	0.6	0.89	14.62
11	U	400	2	25	3.01	0.3	0.89	5.67
12	U	400	2	25	3.01	0.15	0.86	9.19[d]
13	U-10Fe	800	2	25	3.00	0.3	0.76	3.50[d]
14	U-10Fe	800	2	25	3.00	0.9	0.86	3.96[d]

a. U mp = 1133 C, U-10Zr liquidus temp. = 1360 C, U-5Zr liquidus temp. = 1251 C, and U-10Fe eutectic mp = 725 C.

b. Excludes frozen jet portion.

c. Mean diameter = $1/\sum_{i}[(\text{weight fraction})_i/dp_i]$.

d. Excludes agglomerated material.

Particle size decreased with increased duration of the hydrodynamic action on the pour stream before freezing. The largest particles were obtained from the tests with a low melt temperature. In a test in which the melt furnace was pressurized to give an injection velocity of 10 m/s the pour stream was dispersed into smaller particles (mean size of 0.59 mm) and a lower voidage (0.84) than the low velocity tests in which the pour stream was accelerated by gravity to about 2 m/s.

In order to determine the hydrodynamic breakup length and impingement heat flux, tests were conducted with uranium metal pours at 400 C superheat and progressively decreasing sodium depths from 0.9 to 0.15 m. For sodium depths as low as 0.3 m the uranium pour stream broke up and the fragments solidified before reaching the bottom of the interaction vessel. The 0.3-m depth was sufficient for solidification of only a thin (~1 mm) discontinuous crust of the molten U which formed on the base plate. With a sodium depth of 0.15 m the uranium was not completely solidified before impacting the bottom of the vessel. An agglomerated mass was formed on the stainless steel base plate. This mass was not fused to the base plate but came off in one piece (see Fig. 2).

In the tests with U-10 wt% Fe eutectic mixture the melt was heated to the same temperature (1530 C) as the uranium but was 800 C above the eutectic melting point (725 C). As a result in the test with a 0.3-m sodium depth the pour stream material was not completely frozen when contacting the base plate. An agglomerated mass weighing approximately 2.6 kg froze to the base plate and could not be readily removed as the uranium agglomerates. The voidage was still quite high at 0.76. In the next test with the iron eutectic the sodium depth was increased to 0.9 m. The somewhat smaller mean particle size (4 mm) resulting from this test is attributed to the longer period for hydrodynamic breakup resulting from the high superheat. The particles tended to have their edges rounded with less evidence of filament formation. The particle shape may be characteristic of the alloy material as well as the extended time for freezing. The bed voidage was again quite high at 0.86. The particles were not entirely solidified when they reached the base plate. A small agglomerate formed which adhered to the base plate (see Fig. 3). It is of interest to note that the agglomerates formed in the tests with the iron alloy fused into the steel base plate, whereas the particle agglomerates of

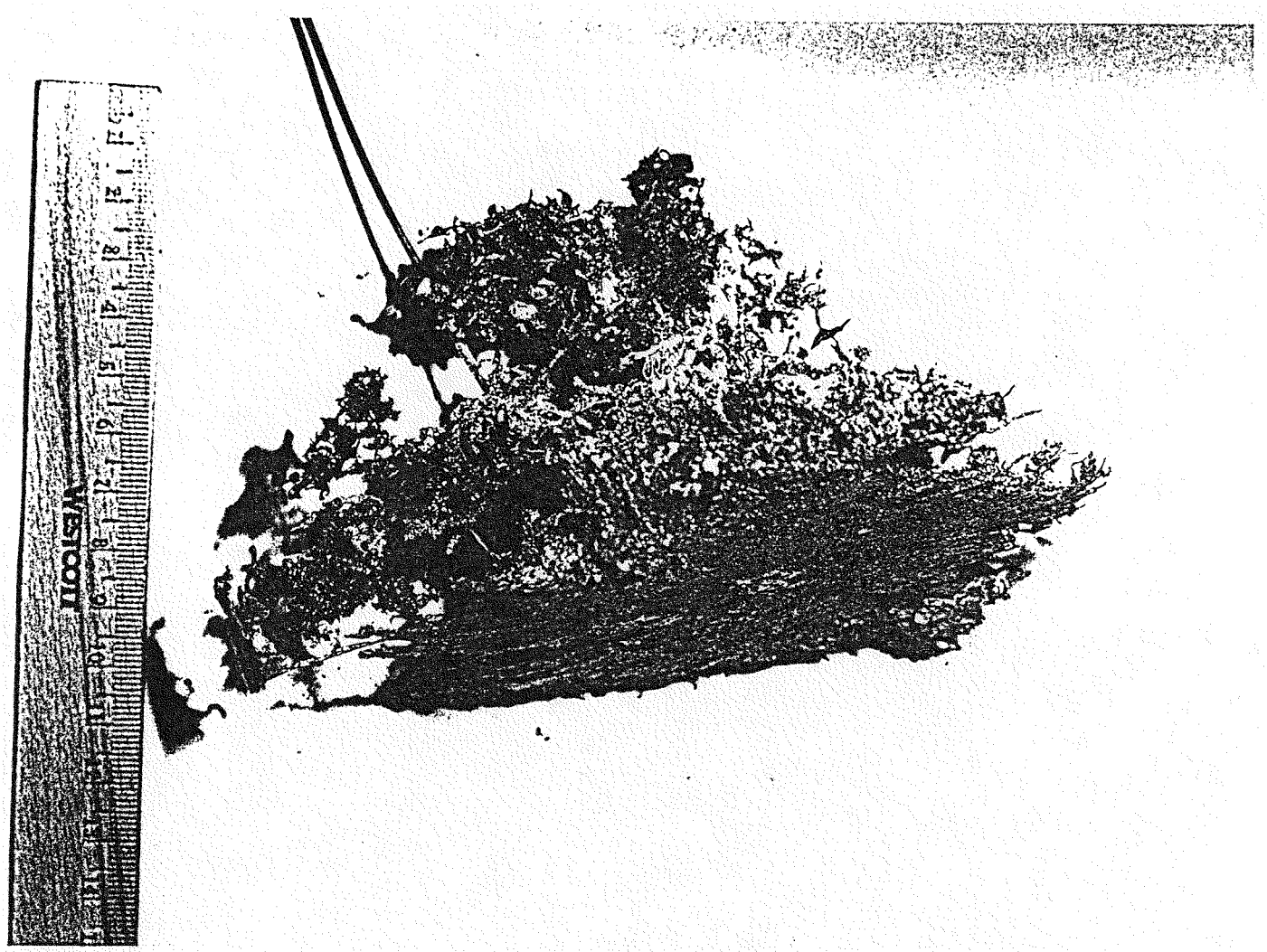

Fig. 2. Sintered Uranium Particle Agglomerate.

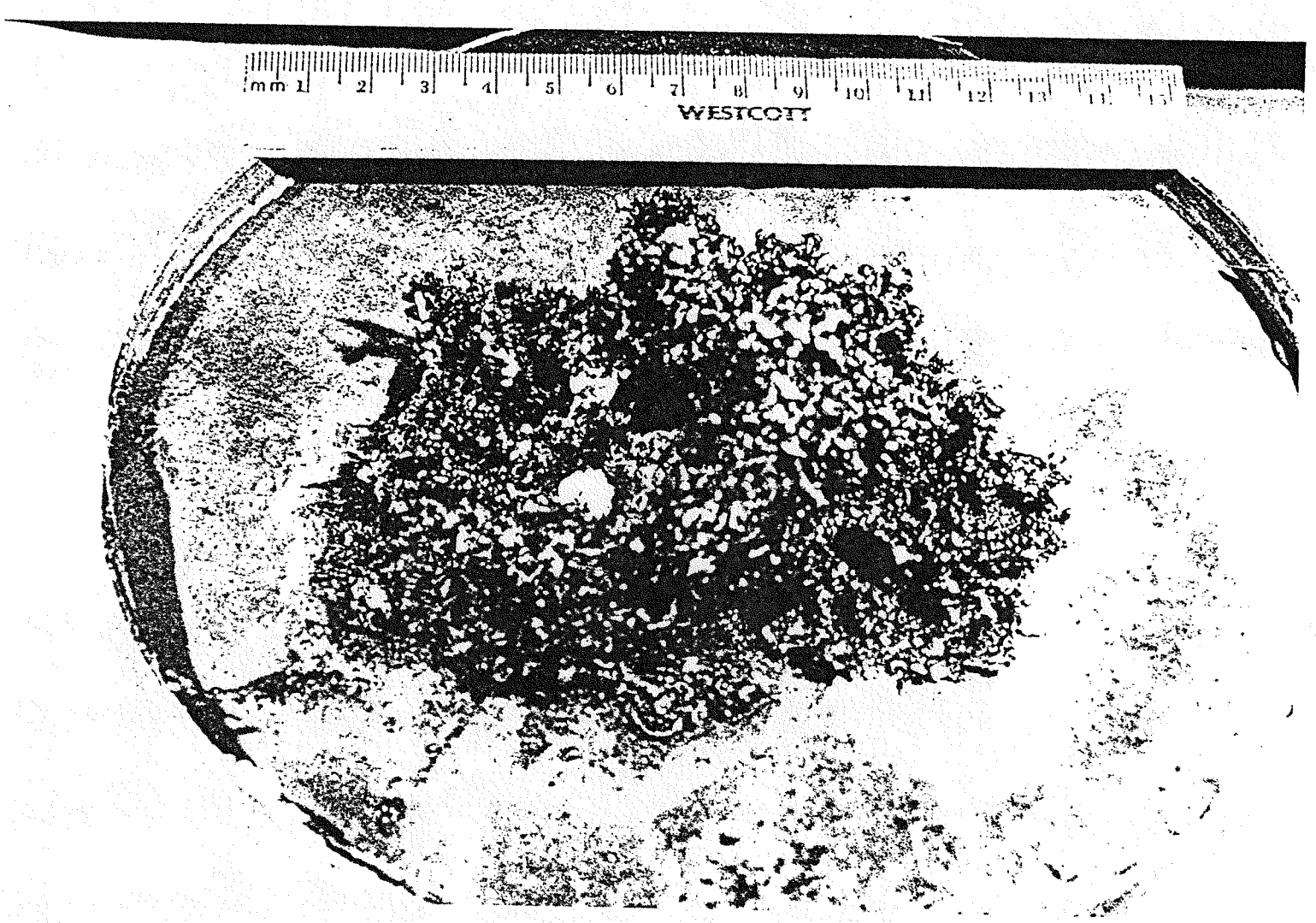

Fig. 3. Agglomerate of U-10 wt% Fe Fused to Base Plate.

pure uranium did not adhere. This may be indicative of the high potential for melt attack on steel structures by a uranium-iron alloy.

Temperature Response of Base Plate

Radiographs as well as direct observations of the material deposited on the base plate revealed that in the cases when the fragments agglomerated on the base plate there remained considerable voidage. Therefore analysis of the temperature response must take into account the two-phase nature of the hot debris. An analysis was made of the observed response in order to interpret the mechanisms involved and to provide a basis for calculations for specific cases in reactor accident analysis.

The analysis made was based on a two-step process: (1) determination of the temperature of the interface between the particle bed and the steel base plate on contact, and (2) determination of the interior temperature response of the steel base plate using the calculated interface temperature. Calculations were based on the simplifying assumption of two semi-infinite solids at uniform but different initial temperatures coming together in perfect contact. On this basis the mutual interface temperature immediately assumes a steady value of T_i.[14]

$$T_i = T_1 + \frac{T_2 - T_1}{1 + \sqrt{\rho_1 C_1 K_1 / \rho_2 C_2 K_2}} \qquad (1)$$

The subscripts 1 and 2 refer to the steel and particle of density, ρ, heat capacity, C, and thermal conductivity, K, bed properties, respectively. The properties used in these calculations are given in Table 2.

The Kampf-Karsten[15] model is an appropriate estimate of the thermal conductivity for a media with a highly conductive fluid phase and ill defined shapes for the solid phase.

$$K_2 = K_{Na}\left[1 - \frac{(1-\varepsilon)(K_{Na}/K_U - 1)}{1 + (1-\varepsilon)^{1/3}(K_{Na}/K_U - 1)}\right] \qquad (2)$$

TABLE 2. Properties Used in Temperature Response Calculations

Material	ρ, kg/m^3	C, J/kgK	K, W/mK
Sodium	769.8	1.262×10^3	55.55
Uranium	17,500	0.161×10^3	54.7
Steel	7,600	0.6276×10^3	20.92

The other particle bed properties can be estimated by volume averaging the fractions of the sodium and uranium phases resulting in:

$$\rho_2 C_2 K_2 = [\varepsilon(\rho C)_{Na} + (1 - \varepsilon)(\rho C)_U]K_2 \tag{3}$$

However, for this case, in which the thermal conductivities of the solid and the fluid phases are nearly the same, a simple volume average of all the properties,

$$\rho_2 C_2 K_2 = \varepsilon(\rho CK)_{Na} + (1 - \varepsilon)(\rho CK)_U \, , \tag{4}$$

resulted in no difference in the calculated interface temperature. It is recommended that the Kampf-Karsten model or some other appropriate correlation be used if the particulate material such as an oxide would have a significantly different thermal conductivity than the fluid phase.

The temperature response of the steel base is[14]

$$\frac{T - T_1}{T_i - T_1} = 1 - \text{erf} \frac{X}{2\sqrt{a_1 t}} \tag{5}$$

where T refers to the steel temperature at position X at time t and α_1 is the

thermal diffusivity ($K/\rho C$) of the steel. The experimental temperature responses were compared to the values determined from the above equations.

It must be noted that Eqs. 1 and 5 have been found to be inappropriate for describing heat transfer after short contact times between a continuous solid media and a gas-solid particle bed.[16] This is because the temperature responses of the individual phases in a gas-solid media greatly differ and cannot be described as a homogeneous media with an effective thermal conductivity as implied with the use of Eqs. 1 and 5. However, when a gas-solid bed with particles of size d has resided on the solid surface for times at which the parameter $t/d^2 > 2\text{x}10^7$ s/m^2, Eqs. 1 and 5 would apply since the thermal front has penetrated sufficiently so that the particle bed can be described in terms of average properties. However, for the present case of a sodium-uranium particle bed in which the thermal conductivities of the two metals (Table 2) are the same and there is a predominate fraction of one phase (sodium), average properties can be used with little error. Also for the tests reported here, measurement of the particle bed temperature profile was not made and only the response of the solid steel base plate was monitored.

The initial temperature of the base plate in run 11 was 606 C before contact with the particles (see Fig. 4). The thermocouple (TC-19) located on the top surface of the base plate peaked at 1000 C, which was taken as the initial particle bed temperature. The subsequent decline in temperature was arrested at 2.5 s after contact for a period of 1.5 s at 760 C, which was taken as the experimental interface temperature. For this test with ε = 0.887, $\rho_2 C_2 K_2$ is estimated from Eq. 4 to be 6.53×10^7 J^2/M^4K^2 s. The interface temperature is calculated to be 782 C from Eq. 1 using this value for the particle bed. This calculated interface temperature is comparable to the observed 760 C temperature arrest.

The steel temperature response was determined from Eq. 5 and compared with the responses of the thermocouples located 6.35, 12.7, and 19.05 mm below the surface. The calculated temperatures shown in Fig. 4 are based on the observed interface temperature (760 C). If, for example, the calculated interface temperature (782 C) were used, after 5 s the temperature 6.35 mm below the surface would be 665 C compared to 658 C with the use of a 760 C interface temperature. The responses of the three thermocouples in the base plate and the thermocouple on the surface are combined in Fig. 4. The data

are compared with this simple model for the temperature response.

It is seen on Fig. 4 that the calculated temperature response of the steel base plate is in fairly good agreement with measured response for about the first 5 s. The calculated temperatures eventually become higher than the measured response with the greatest deviation for the thermocouple located 6.35 mm below the surface. One reason for this deviation is the assumption of two semi-infinite media with no lateral heat transfer. Also the calculations are based on a constant interface temperature, whereas actually the interface temperature as indicated by TC-19 declined, and the effect of the heat of fusion was not considered. Because of these effects it was not meaningful to carry the calculations beyond 12 s.

In Run 12 with only a 0.15-m sodium depth the particles were not completely solidified when they reached the bottom and sintered to form an agglomerate. The observed interface temperature of 765 C (Fig. 5) based on the arrest in temperature decline of the thermocouple on the base plate surface was used in the temperature response calculations. The calculated interface temperature of 760 C was in close agreement with observed interface temperature. The calculated interface temperature was determined from Eqs. 1 and 4 using values of 945 C for T_2, 608 C for T_1 and a particle bed voidage of 0.86. The initial temperature profile across the base plate with temperatures of 608 C, 611 C, and 595 C was not as uniform as for Run 11. The temperature changes at each position were calculated relative to its initial temperature. Again the calculated response at the point 6.35 mm below the surface exceeds that recorded from the thermocouple because of the assumptions. However, the agreement of 12.7 and 19.05 mm below the surface is excellent.

In Run 13, also conducted with a 25-mm thick base plate, the thermocouple located 12.7 mm below the surface failed. The thermocouples at 6.35 and 19.05 mm indicated initial temperatures of 608 C and 588 C respectively. Because of this considerable temperature deviation within the steel plate no attempt was made to compare experimental and calculated values using the present model. However, on the basis of Runs 11 and 12 the calculational technique used does indicate that impingement heat flux is amenable to calculation and, that with appropriate boundary conditions, can be extended to reactor safety analysis for metal fuels.

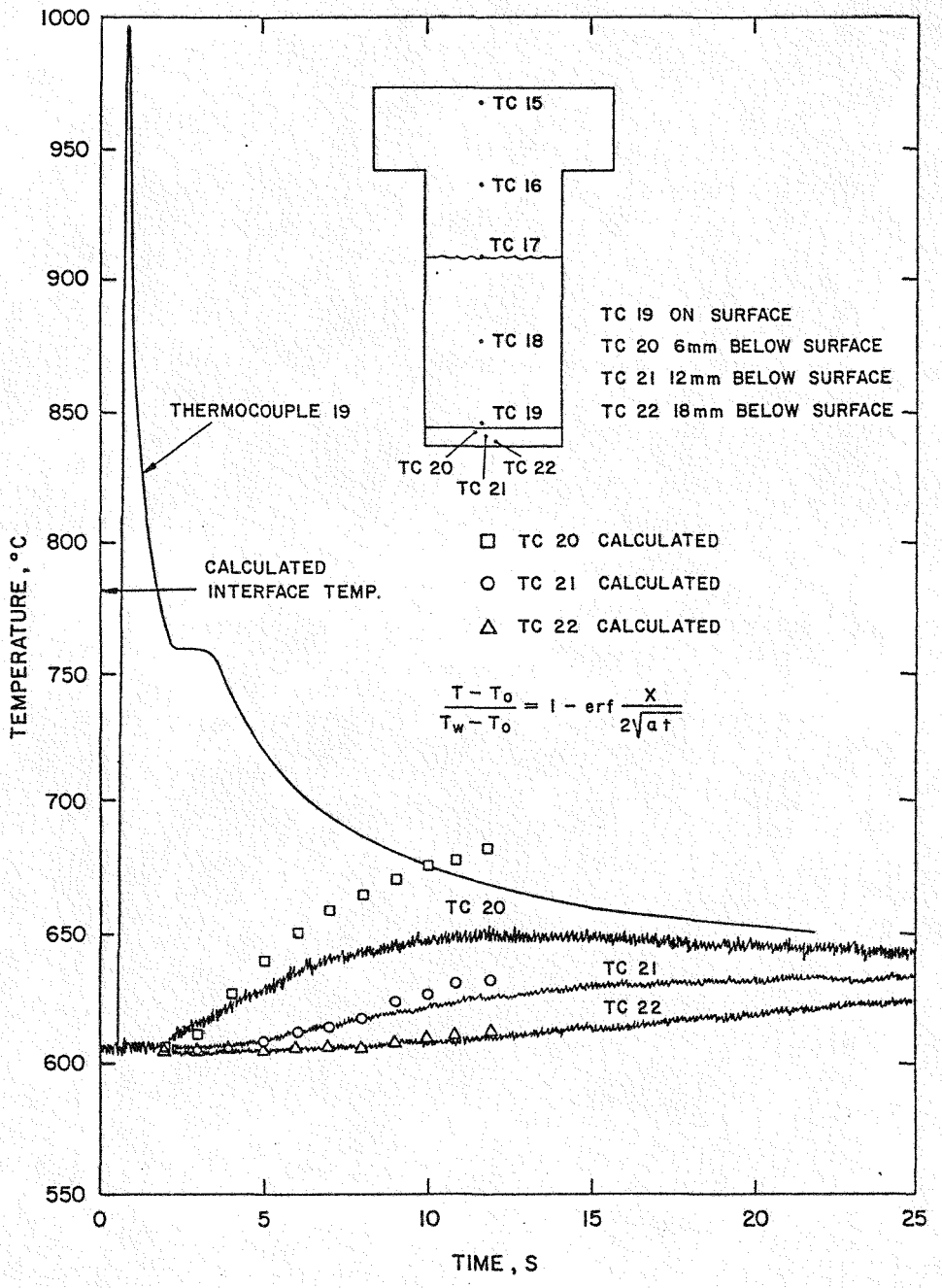

Fig. 4. Temperature Response of Base Plate for Run 11; U metal, 0.3 m sodium depth

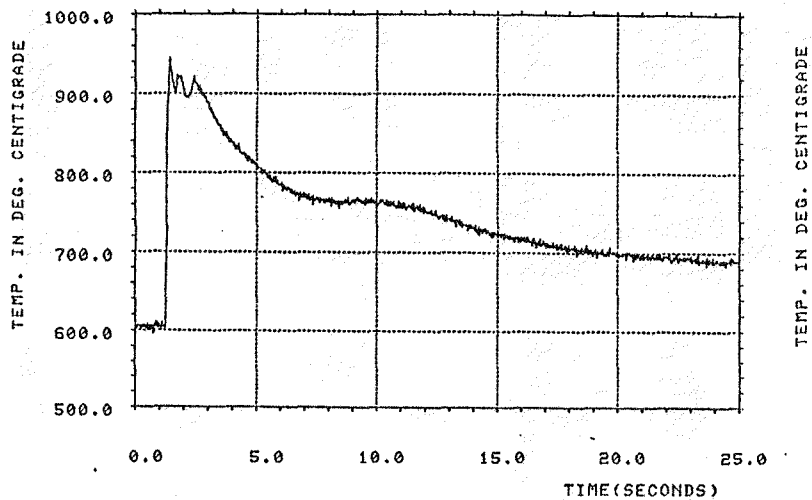

a. Thermocouple on surface

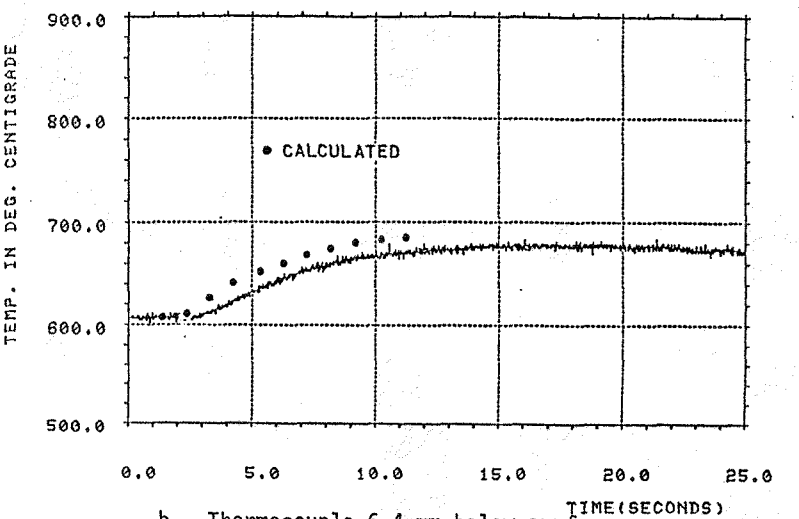

b. Thermocouple 6.4 mm below surface

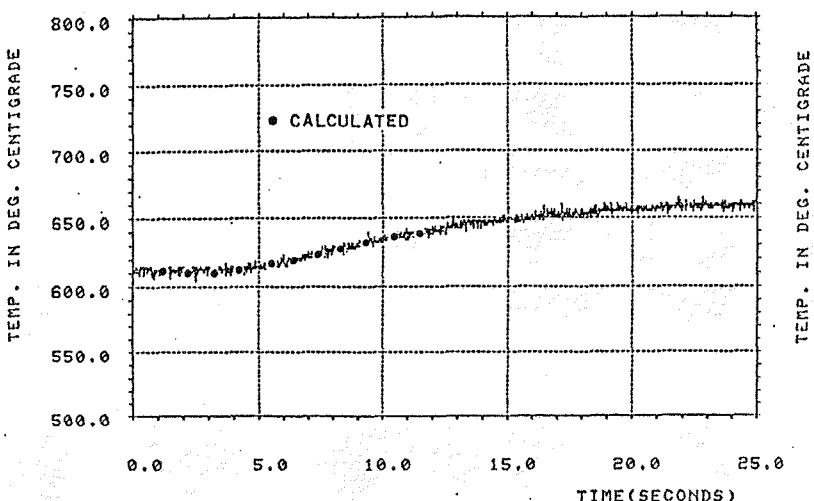

c. Thermocouple 12.7 mm below surface

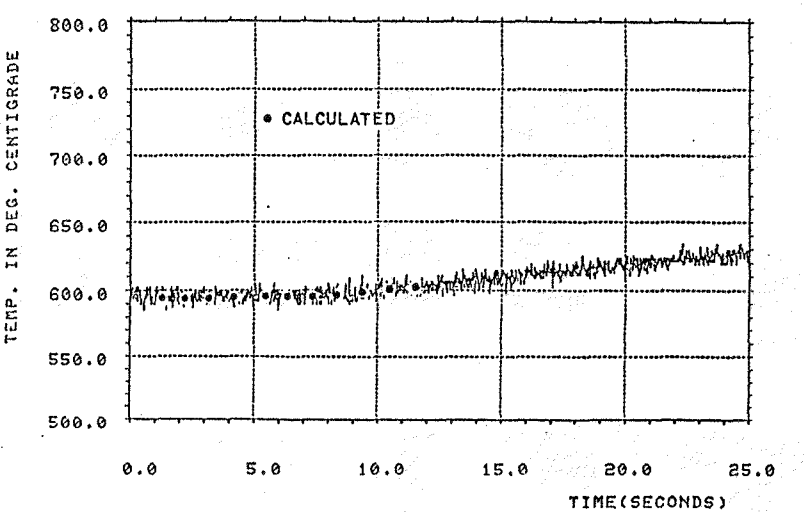

d. Thermocouple 19.1 mm below surface

Fig. 5. Temperature Response of Base Plate for Run 12 ; U metal, 0.15 m sodium depth

Conclusions

1. A sodium depth of less than 0.3 m was required for complete hydrodynamic breakup and freezing of the 25-mm diameter uranium pour stream.

2. The U-10 wt% Fe particles were somewhat rounder and smaller (mean size ~4 mm) because the higher superheat for this uranium-iron alloy melt permitted more hydrodynamic action before freezing.

3. The sintered agglomerates of uranium particles did not adhere to the base plate while the U-10 wt% Fe alloy agglomerates fused into the base plate.

4. The temperature response of the 25.4-mm steel base plate on impingement of the particle bed was in reasonable agreement with a simple model based on semi-infinite mediums and average properties for the particle bed.

5. The base plate temperature 6.3 mm below the surface rose after contact with the pour stream material to a maximum of only 670 C for the most severe test with an 0.15-m sodium depth. While there was no contribution by decay heat in these tests, it does appear that the rise in base plate temperature will be moderate and that it would be possible to arrest the accident if heat removal from the sodium can be maintained because of the high voidage of the particle bed. It is recognized that it is necessary to keep the U-Fe alloy below its melting point to prevent further degredation of the base.

References

1. D. L. Swift and L. Baker, Jr., "Experimental Studies of the High-temperature Interaction of Fuel and Cladding Materials with Liquid Sodium," ANL-7120, Argonne National Laboratory (1965).

2. B. W. Spencer, L. M. McUmber, D. Gregorash, R. W. Aeschlimann, and J. J. Sienicki, "Corium Quench in Deep Pool Mixing Experiments," Trans. 23rd Natl Heat Trans. Conf., Denver, CO, August 1985.

3. T. R. Johnson, J. R. Pavlik, and L. Baker, Jr., Unpublished information, 1974.

4. R. E. Henry, J. D. Gabor, I. O. Winsch, E. A. Spleha, D. J. Quinn, E. G. Erickson, J. J. Heiberger, and G. T. Goldfuss, "Large Scale Vapor Explosions," Proc. Fast Reactor Safety Mtg, Beverly Hills, CA, CONF-740401-P2, p. 922, April 1974.

5. B. W. Spencer, J. D. Gabor, J. C. Cassulo, and D. J. Kilsdonk, "Results of Scoping Experiments on Melt Stream Breakup and Quench," Proc. Intl ANL/ENS Topical Mtg. on Thermal Reactor Safety, ANS 700106, San Diego, CA, Feb. 2-6, 1986.

6. K. Hartel and K. Martin, "Ein Rechenmodell zur Bestimmung der Hydrodynamischen Stabilitat van Flussigketis-Freistrahlen in Flussigkeit," KfK 3978, Kernforschungszentrum Karlsruhe (1986).

7. B. W. Spencer, J. D. Gabor, and J. C. Cassulo, "Effect of Boiling Regime on Melt Stream Breakup in Water," Proc. 4th Intl Symp. on Multi-Phase Transport and Particulate Phenomena, Miami Beach, FL, December 1986.

8. M. Berman, N. A. Evans, and M. S. Krein, "Core Melt/Coolant Interactions: Experiments," NUREG/CP-0048, Sandia National Laboratories, pp. 218-225, October 1983.

9. K. Miyazaki, K. Morimoto, O. Yamamoto, Y. Harada, and N. Yamoka, "Thermal Interaction of Water Droplet with Molten Tin," J. Nucl. Sci. Tech., 21, pp. 907-918 (1984).

10. J. J. Sienicki and B. W. Spencer, "The Jet Impingement Phase of Molten Core-Concrete Interactions," Proc. of the Committee on the Safety of Nuclear Installations (CSNI) Specialists' Meeting on Core Debris-Concrete Interactions, EPRI NP-5054-SR, pp. 4-29-4-47, February 1987.

11. M. Epstein, M. J. Swedish, J. H. Linehan, G. A. Lambert, G. M. Hauser, and L. J. Stachyra, "Surface Ablation in the Impingement Region of a Liquid Jet," AIChE Journal, 25, p. 630 (1979).

12. J. D. Gabor, R. T. Purviance, R. W. Aeschlimann, and B. W. Spencer, "Characterization of IFR Metal Fuel Fragmentation," Trans. Am. Nucl. Soc., 54, pp. 251-253 (June 1987).

13. J. D. Gabor, R. T. Purviance, R. W. Aeschlimann, and B. W. Spencer, "Breakup and Quench of Molten Metal Fuel in Sodium," Proc. Am. Nucl. Soc. Safety of Next Generation Power Reactors Mtg., Seattle, pp. 838-843, May 1-5, 1988.

14. W. M. Rohsenow, J. P. Hartnett, and E. N. Ganic, Ed., Handbook of Heat Transfer Fundamentals, Second Edition, McGraw-Hill, New York, pp. 4-80 - 4-83, 1985.

15. H. Kampf and G. Karsten, "Effects of Different Types of Void Volumes on the Radial Temperature Distribution of Fuel Pins," Nucl. Appl. Tech., 1, pp. 288-300 (1970).

16. J. D. Gabor, "Wall-to-bed Heat Transfer in Fluidized and Packed Beds," Chem. Eng. Progr. Symp. Series No. 105, 66, pp. 76-86 (1970).